JOURNAL OF CATALYSIS 53, 266–279 (1978)

Rates and Coverages in the Low Pressure Pt-Catalyzed Oxidation of Carbon Monoxide[1]

A. GOLCHET AND J. M. WHITE

Department of Chemistry, University of Texas, Austin, Texas 78712

Received December 2, 1977; revised February 13, 1978

The Pt-catalyzed oxidation of CO has been investigated using polycrystalline foil over the temperature range 375 to 1000°K and pressures between 10^{-6} and 10^{-3} Pa. Emphasis is placed on temperatures between 450 and 550°K, where the steady-state rates are very sensitive to the ratio $p\mathrm{CO}/p\mathrm{O}_2$. At pressures of CO which lie well below the pressure of O_2, the reaction rate is first order in CO pressure, but when the CO pressure lies above the O_2 pressure, the rate is inhibited by CO to an extent which depends on the temperature and oxygen pressure. Coverages of oxygen and carbon monoxide have been determined under working conditions using transient titration and flash desorption techniques. These measurements indicate that the oxygen coverage drops smoothly as CO pressure is increased. The CO coverage is not detectable until the oxygen coverage becomes very small, but once CO begins to accumulate, its concentration rises sharply toward the isotherm value. For temperatures around 475°K and below, the transformation from the first order (in CO) to the inhibition regime is relatively slow and leads to a series of relatively long-lived states which have not been adequately characterized. The steady-state kinetic and coverage data are discussed in terms of a kinetic model which assumes dissociative oxygen chemisorption and a mobile carbon monoxide precursor state.

INTRODUCTION

As a part of continuing effort to characterize in detail the kinetics of the oxidation of carbon monoxide on transition metals, we report here measurements of steady-state rates and coverages at low total pressures (10^{-6} to 10^{-3} Pa) with particular attention to a set of striking transitions from high to low CO_2 production rates, which are observed for small variations in $p\mathrm{CO}/p\mathrm{O}_2$ in the temperature region below 540°K. By means of chemical titration and flash desorption techniques, coverages of CO and O have been measured for several pressure ratios near the transition region. These data allow us to discuss the variation of the CO_2 production rate with coverage and collision frequency.

The behavior of oxygen and carbon monoxide on Pt has received a tremendous amount of attention. Studies of adsorption, desorption, and reaction have used a wide variety of pressure, temperature, and substrate conditions. Since the results reported here involve relatively low total pressures (10^{-6} to 10^{-3} Pa) and an unsupported substrate, we will refer mainly to low pressure studies on single crystal and polycrystalline substrates in the following introductory comments.

Oxygen adsorption on polycrystalline and single crystal Pt substrates has been studied

[1] This research was supported in part by National Science Foundation Grants CHE75-13732 and CHE 77-07827.

0021-9517/78/0532-0266$02.00/0

using flash desorption (*1–11*), LEED (*10–18*), AES (*10, 17–26*), XPS (*2, 28*), UPS (*2, 22, 23, 28–30*), work function (*1, 30, 32*), FEM (*31, 32*), molecular beams (*33 36, 99*), H_2 and CO titration (*37–40*), and theoretical (*42–45*) techniques. Regardless of the crystallographic orientation, there is general agreement that (1) adsorption is dissociative, except perhaps at temperatures below 300°K,[2] (2) the reactivity of adsorbed oxygen with CO or H_2 is very high except under certain conditions where an oxide-type state is present (*17, 23, 88*), and (3) the initial sticking probability is in the range 0.2 to 0.4 except when the surfaces have few defects and steps, in which case the oxygen sticking probability is smaller (*3, 7–9, 14, 17, 21, 22, 42*).

The chemisorption of CO on Pt has been studied extensively using LEED (*10, 14, 22, 62–67*), work function (*14, 68, 69*), infrared (*71–76*), energy loss (*77*), photoemission (*1, 78–83*), AES (*10, 22, 64, 84–89*), flash desorption (*1, 3, 14, 22, 68, 88–92*), and theoretical (*43, 93*) techniques. In general, there is agreement that (1) adsorption is nondissociative for T less than 600°K, except perhaps at steps and kinks, (2) techniques involving electron beams must be used cautiously because of the tendency to dissociate CO and leave a carbon deposit, (3) the heat of adsorption at low coverage is around 30 kcal $mole^{-1}$, and (4) the initial sticking coefficient is greater than 0.5.

The Pt-catalyzed reaction of CO and O_2 to form CO_2 has been studied using molecular beam (*56–58, 99*), low pressure steady-state (*3, 23, 47–53, 60, 69, 70, 94–98*), low pressure transient (*3, 15, 48–51, 54, 59*), and theoretical (*100*) techniques. The results may be summarized as follows: (1) below 600°K, the reaction between adsorbed CO and gas phase oxygen is very slow, whereas that between gas phase CO and chemisorbed oxygen is fast and first order in CO collision frequency (*23, 59*), (2) it is possible to form a surface oxygen species which is not reactive towards CO (*3, 15, 17–21, 23, 31, 71, 88, 89*), (3) the reaction rate is zero order in oxygen coverage, except at low coverages, which implies that the simple impact Eley–Rideal model is inadequate (*59*), and (4) at temperatures below 500°K, the rate of CO_2 production is inhibited when the carbon monoxide pressure exceeds the oxygen pressure (*47–50*). These observations have usually been interpreted in terms of an Eley–Rideal or a Langmuir–Hinshelwood reaction mechanism. While both of these have some utility, it is useful to look in more detail at the encounters which take place between CO and O to make CO_2. Transient experiments at 550°K on (111), stepped (111), and polycrystalline surfaces have proven very useful in this enterprise (*15, 24, 25, 59*). At lower temperatures, near 475°K, the accumulation of CO becomes important, and detailed low pressure kinetic studies in this region have not been made. It is to this end that the work reported here has been carried out.

EXPERIMENTAL METHODS

The experimental apparatus and procedures were nearly the same as described earlier (*59*), so only a brief description will be presented here. A standard ion-pumped vacuum system operating at base pressures around 3×10^{-7} Pa was used. The major residual was CO, and care was taken to keep the hydrogen background below 10^{-8} Pa. Partial pressures were measured with a quadrupole mass spectrometer, taking into account the fragmentation patterns and sensitivities for various species. Total pressures were determined using a Bayard-Alpert ionization gauge and literature

[2] For experimental arguments favorable to the assumption of a dissociative adsorption of oxygen see Refs. 2, 5, 9, 10, 22, and 39. Dissociative adsorption, however, has also been assumed in Refs. 4, 6, 7b, 19, 27, and 40 through 52 at UHV conditions and in Ref. 37 at relatively high pressures.

values for relative sensitivities (*102*). During both steady-state and transient kinetic measurements, the systen was continuously pumped, and reagents were introduced through two leak valves. The pumping speed for CO_2 was 2.7 ± 0.2 liters sec^{-1}. Steady-state rates were recorded only after the system had stabilized at constant values of pCO, pO_2, pCO_2, and T for at least 15 min. In certain cases outlined below, this time may be insufficient to allow surface concentrations to stabilize.

A relatively large area of polycrystalline platinum foil ($0.75 \times 4 \times 0.009$ cm; 99.99% purity) was used in order to minimize the relative significance of background CO_2 production at the walls and hot filaments. For all the experiments reported here, background CO_2 production was measured and subtracted from total measured rates. The Pt foil was spot-welded to short lengths of 0.052-cm-diam Pt wire, which in turn were spot-welded to 0.23-cm-diam tungsten rods which served as current leads for resistive heating. A calibrated Pt/Pt–13% Rh thermocouple was spot-welded to the center of the substrate. Temperatures were controlled to within ± 1°K in the 300 to 500°K range using an electronic circuit. At 1000°K, no temperature gradient across the 4-cm length of the substrate was detected with an optical pyrometer.

The Pt sample was pretreated by heating at 1450°K in 10^{-4} Pa of O_2 for more than 5 hr. This treatment establishes stable catalyst behavior, as indicated by reproducible steady-state CO_2 production rates and flash desorption spectra of CO and O_2. The latter agree with spectra from surfaces which were clean according to Auger spectra (*10*). Daily pretreatments at 1000°K (roughly 10^{-4} Pa of O_2 for 15 min) were used to reduce carbon contamination. Heating Pt in O_2 at 1000°K produces two kinds of oxygen, which can be distinguished by AES (*18–20, 23*), LEED (*17, 18*), and reactivity towards CO (*17, 23, 88, 89*). For the particular foil used here, AES (*23*) showed that nonreactive oxygen formed slowly around 1000°K and was destroyed by heating to above 1200°K and that the presence of small amounts of this oxygen did not alter qualitatively the behavior of reactive oxygen. The experiments reported here must therefore be regarded as involving small and unknown amounts of nonreactive oxygen, produced during both pretreatment and reaction studies, and distributed in an unknown way in the subsurface region. The extent to which this oxygen controls the rate is not known quantitatively; however, the catalyst activity and CO desorption spectra were very reproducible, even with wide variations in the oxygen pressure and time used in the daily pretreatments. These observations, combined with the AES data, suggest that the nonreactive oxygen concentration in the surface region was small and had, at most, a minor effect on the rate measurements reported here.

Carbon monoxide coverages were determined both in the presence and absence of O_2 by establishing a steady-state condition and then flash heating the substrate at ~ 30°K sec^{-1} while monitoring the CO pressure as a function of time. Reactive oxygen coverages were determined using the transient CO pressure-jump and the oxygen pressure-jump methods (*59*). These use the integral of the transient CO_2 production, which arises from the reaction of CO with chemisorbed oxygen atoms, as a measure of the oxygen coverage.

Steady-state results were independent of the ionization gauge filament condition, but some of the transient experiments involving observation times of several minutes were not. Therefore, the ionization gauge was turned off during transients to minimize this effect, which apparently arises because the ionization gauge filament is a source for the supply of oxygen atoms to the surface. With the ion gauge off, the

measured areas under transient CO_2 titration curves were nicely reproducible.

RESULTS

Temperature Dependence of Steady-State CO_2 Production Rates

Steady-state CO_2 production rates were measured over the temperature range 370 to 1070°K for four fixed gas phase conditions: (1) $p(O_2) = p(CO) = 1.33 \times 10^{-5}$ Pa; (2) $p(O_2) = 5$, $p(CO) = 6.65 \times 10^{-5}$ Pa; (3) $p(O_2) = 10$, $p(CO) = 1.33 \times 10^{-4}$ Pa; and (4) $p(O_2) = 0.2$, $p(CO) = 1.33 \times 10^{-5}$ Pa. The results are shown in Fig. 1 as the logarithm of the rate per unit pressure of O_2 and CO versus the inverse of temperature. This graph has several important features. As often noted in the literature (*48, 103–105*), each curve is volcano shaped,

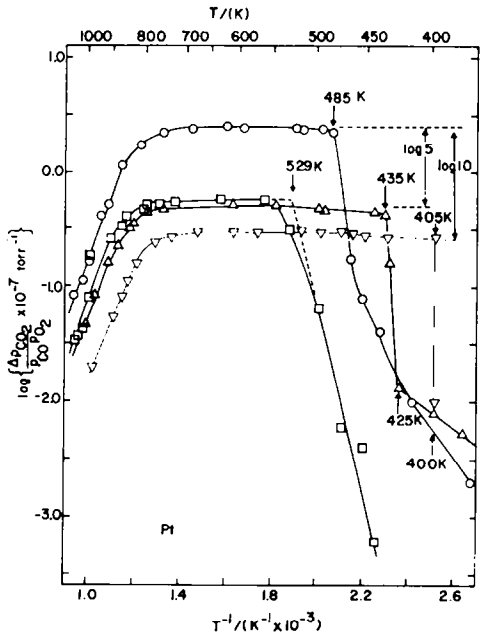

FIG. 1. Arrhenius plot of the CO_2 production rate (normalized to unit CO pressure and unit O_2 pressure) for four pressure conditions: (○) $p(O_2) = p(CO) = 1.33 \times 10^{-5}$ Pa; (△) $p(O_2) = 5p(CO) = 6.65 \times 10^{-5}$ Pa; (▽) $p(O_2) = 10p(CO) = 1.33 \times 10^{-4}$ Pa; (□) $p(O_2) = 0.2p(CO) = 1.33 \times 10^{-5}$ Pa. The arrow on each curve marks the low temperature onset of the region of maximum rate.

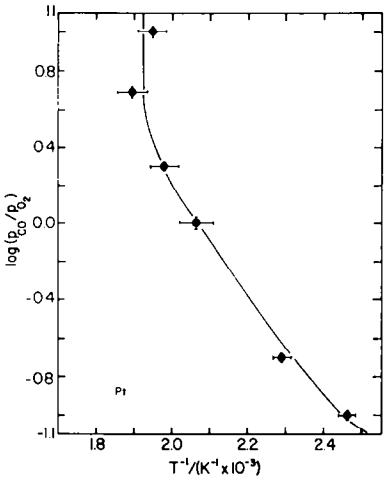

FIG. 2. Logarithm of the ratio pCO/pO_2 as a function of the temperature required to reach the maximum rate.

with a rate maximum at intermediate temperatures. In the intermediate region, the rate is relatively constant over a range of temperatures, the breadth of which depends strongly upon the ratio of O_2 to CO. In general, the breadth increases with increasing pO_2/pCO, and the variations are the result of changes in the lower temperature onset. To within about 10°K this temperature is well defined and increases from 405 to 530°K as the pCO/pO_2 ratio increases from 0.1 to 5. Figure 2 shows how the pCO/pO_2 ratio is related to the temperature required to reach the maximum rate. When pCO/pO_2 is greater than 2, this temperature becomes constant at about 530°K. The temperature required to reach the maximum rate is not very sensitive to the total pressure: raising the total pressure from 1.2×10^{-4} to 2.6×10^{-4} Pa while keeping pCO/pO_2 equal to 10 produces very little change in its value. Over the pressure range accessible in our experiments, 1.3×10^{-6} to 1.3×10^{-3} Pa, this result is general: the pressure ratio rather than the total pressure determines the temperature required to reach the maximum rate. For pO_2/pCO equal to or greater than 10, some sensitivity to total pressure may

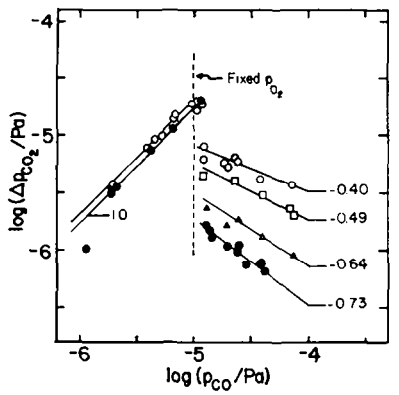

FIG. 3. Steady state CO_2 production rates as a function of CO pressure for a fixed O_2 pressure of 10^{-5} Pa. The temperatures are (●) 453°K, (△) 463°K, (□) 473°K, and (○) 485°K. Kinetic orders in CO pressure are shown for each curve.

occur. We have not, however, systematically investigated this point. The high temperature at which the rate begins to drop on the other hand, is, relatively insensitive to the pO_2/pCO ratio and occurs near 775°K. Between 850 and 1050°K, the temperature dependence of the rate is characterized by an apparent activation energy of -105 ± 2 kJ mole^{-1}, independent of the gas phase concentration.

The temperature dependence at low temperatures, unlike that at intermediate and high temperatures, is a sensitive function of the gas phase composition. For pCO/pO_2 equal to 5, the apparent activation energy is 140 ± 5 kJ mole^{-1} over the range 450 to 530°K. The apparent activation energy decreases sharply as pCO/pO_2 decreases and is about 30 kJ mole^{-1} when pCO/pO_2 is equal to 0.2.

A further important feature of the data in Fig. 1 is the very sharp increase in the rate which occurs at about 400°K for pCO/pO_2 equal to 0.1 and at 425°K for pCO/pO_2 equal to 0.2. There is a hint of such a break at about 460°K for pCO/pO_2 equal to 1, but for pCO/pO_2 equal to 5, no sharp increase is found.

Dependence of the Rate on Partial Pressure.

To determine the dependence of the rate on partial pressure, steady-state experiments were done in which pO_2 and temperature were held constant while pCO was varied from low to high values. Examples are shown in Figs. 3, 4, and 5, where the logarithm of the rate is shown as a function of the logarithm of the CO pressure. In each of these figures, the order with respect to the gas phase carbon monoxide pressure is indicated for each linear segment, and the ordinates have all been corrected for

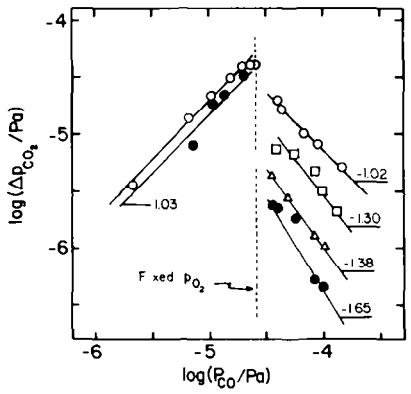

FIG. 4. Steady-state CO_2 production rates as a function of CO pressure for a fixed O_2 pressure of 2.6×10^{-5} Pa. The temperatures are (●) 453°K, (△) 463°K, (□) 473°K, and (○) 485°K. Kinetic orders in CO pressure are shown for each curve.

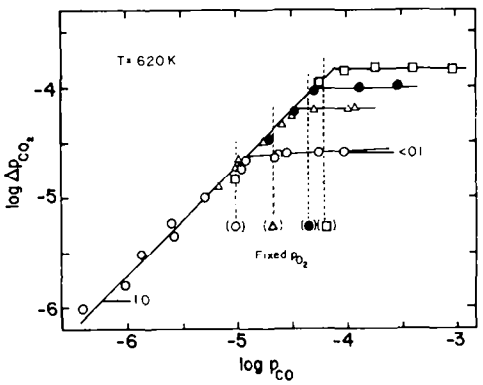

FIG. 5. Steady-state CO_2 production rate as a function of CO pressure for four fixed O_2 pressures at 620°K. The four fixed O_2 pressures are (○) 10^{-5} Pa, (△) 2.66×10^{-5} Pa, (●) 1.66×10^{-5} Pa, and (□) 6.2×10^{-5} Pa.

background CO_2 production. For $p(CO)$, $p(O_2)$ less than 1, the rate is first order in $p(CO)$ for any temperature we used (450–620°K). When $p(CO)$ equals $p(O_2)$, the order changes sharply, and in some cases (T less than 485°K) the rate undergoes a precipitous drop for a very small increase in the carbon monoxide pressure. Additional data regarding this gap region are presented below, where it is noted that some of the points near $p(CO)$ equal to $p(O_2)$ on the first-order portions of Figs. 3 and 4 tended to be unstable. For $p(CO)$ greater than $p(O_2)$, the rate at low temperatures is inhibited by increasing CO. As the temperature is increased to about 540 K, however, the gap disappears, and the inhibitory effect of CO becomes much weaker (Fig. 8). This temperature is very close to the highest of the low temperature onsets shown in Figs. 1 and 2. Thus, lowering the temperature has, under certain conditions, the same precipitous effect on the rate as raising the CO pressure. As discussed below, these effects are related to the accumulation of adsorbed CO at the surface.

For $p(CO)$ less than $p(O_2)$, Fig. 5 shows that the rate is independent of the oxygen pressure (see also Figs. 6 and 7), and Figs. 3 through 5 show that the rate is nearly independent of temperature. This is, of course, directly plotted in Fig. 1. For $p(CO)$ greater than $p(O_2)$, the inhibition effect shown in Figs. 3 through 5 is a strong function of the temperature and the pressure. The gap magnitude and the order with respect to CO (in the inhibition region) both decrease as the temperature increases from 450 to 550°K. As the temperature is increased above 550°K, the order with respect to CO stays near zero but increases slowly. For example, the order is 0.1 for T equal to 620°K, $p(CO)$ greater than $2p(O_2)$, and $p(O_2)$ equal to 10^{-5} Pa. As the oxygen pressure increases, the order seems to move toward zero, but our data do not permit a strong statement. At low temperatures, the effect of increasing the O_2 pressure is to decrease

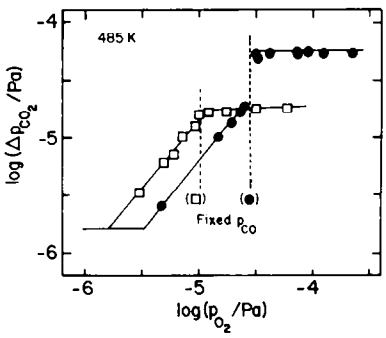

FIG. 6. Steady-state CO_2 production as a function of O_2 pressure at 485°K for two fixed CO pressures. The fixed CO pressures are (□) 10^{-5} Pa and (●) 2.66×10^{-5} Pa.

the order with respect to CO. For example, examining Figs. 3 and 4 at 453°K shows that the order decreases from −0.73 to −1.65 when $p(O_2)$ increases from 1×10^{-5} to 2.6×10^{-5} Pa, while at 485°K it decreases from −0.40 to −1.02.

Similar experiments at 485 and 620°K, except holding $p(CO)$ constant while varying $p(O_2)$, are shown in Figs. 6 and 7. For $p(O_2)$ less than $p(CO)$, the rate is near first order; when $p(O_2)$ is approximately equal to $p(CO)$, the rate changes suddenly and becomes near zero order in $p(O_2)$. Just as in Figs. 3 and 4, a sharp change in the magnitude of the rate is observed at 485°K for a very small change of the oxygen pressure. At 620°K, as shown in Fig. 7, the rate in the high pressure region joins smoothly to the rate

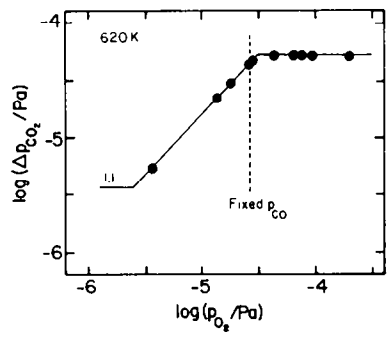

FIG. 7. Steady-state rate of CO_2 production as a function of O_2 pressure at 620°K for a fixed CO pressure of 2.67×10^{-5} Pa.

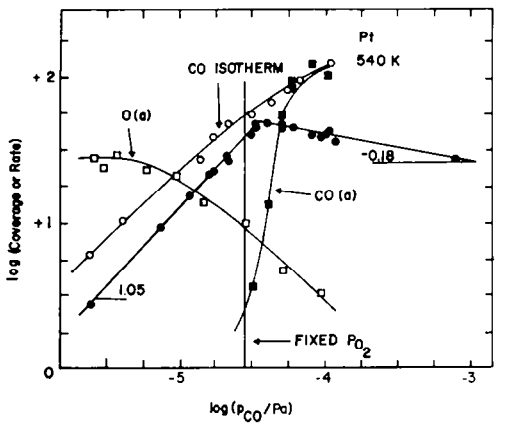

FIG. 8. Combined plot of (●) CO_2 production rate, (□) oxygen coverage (■), carbon monoxide coverage under working conditions, and (○) carbon monoxide isotherm. The oxygen and carbon monoxide coverages are plotted in different and arbitrary coverage units.

in the low pressure region, just as it does when pCO is varied (Fig. 5). Unlike carbon monoxide, oxygen never inhibits the rate.

Coverages of Oxygen and Carbon Monoxide

In order to interpret the observed rates of CO_2 production, it is necessary to obtain coverage data under the working conditions of the catalyst. Figure 8 displays both rate and coverage data as a function of CO pressure at 540°K. The CO isotherm and the adsorbed CO data were determined by flash desorption of a steady-state system at 540°K and known pressure of CO. The isotherm was determined in the absence of gas phase oxygen, and the CO(a) was determined in the presence of 2.7×10^{-5} Pa of O_2. In both cases, the area under the transient CO peak was measured and taken to be proportional to the coverage. Oxygen coverages were determined by the CO_2 decay method (*59*). Areas under the CO_2 decay curves, corrected for the time constant of the system, are plotted in Fig. 8.

As expected, the rate is first order with respect to the pressure of CO for pCO less than $p O_2$. For $p\mathrm{CO}/p\mathrm{O}_2$ equal to 1.3, however, the first-order rate changes smoothly to negative 0.18 order. The coverage of carbon monoxide for pCO less than $p O_2$ is less than 10% of the equilibrium CO isotherm coverage. In this region, the oxygen coverage is relatively high but declines monotonically as the CO pressure increases. As the $p\mathrm{CO}/p\mathrm{O}_2$ ratio of 1.3 is approached from below, the CO coverage under working conditions begins to rise sharply. For example, when the CO pressure is increased from 3.2 to 5.0×10^{-5} Pa, the CO coverage increases by more than an order of magnitude. At even higher CO pressures, the CO coverage approaches the limiting isotherm coverage.

Qualitatively, the same general behavior is observed at 485 and 453°K, as shown in Fig. 9. Only coverage data are shown, the open symbols are for 453°K, and the closed for 485°K. Coverages are normalized to room temperature saturation values determined by flash desorption (CO) and titration (O).

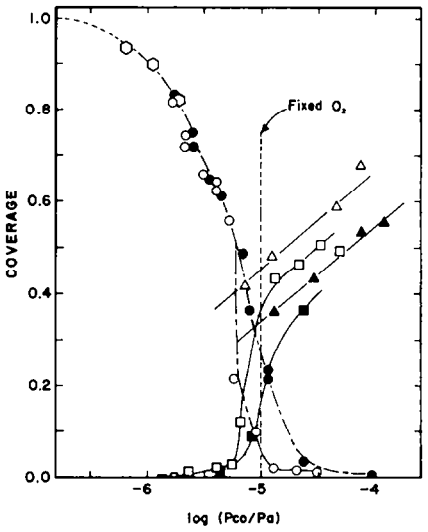

FIG. 9. Combined plot of (circles) oxygen coverages, (squares) carbon monoxide coverages under working conditions, and (triangles) carbon monoxide isotherm coverages. The open and solid symbols refer to 453 and 485°K, respectively. The open hexagons are oxygen coverages determined by the CO pressure jump method, and the circles were determined by the CO_2 decay method.

The open hexagons of Fig. 9 are oxygen coverages determined by the CO pressure jump method (*106*), and the open circles are those determined by the CO_2 decay method. The two methods agree at 1.8×10^{-6} Pa and join together smoothly. The oxygen coverages at 485°K (indicated by solid circles in Fig. 9) are superimposable on the 453°K data when the CO pressure is well below the O_2 pressure. Around 5.6×10^{-6} Pa, however, the two sets of data become distinguishable, the results at 453°K dropping sharply to near-zero coverage at lower CO pressure than at 485°K.

The CO coverages increase sharply from near zero to just below the adsorption isotherm, at pCO approximately equal to pO$_2$. At 453°K, the CO accumulates at lower CO pressure than at 485°K, and, since the isotherm lies at higher coverage, the amount of adsorbed CO is generally higher at 453°K. According to the data of Fig. 9, at 453°K, the CO coverage becomes equal to the oxygen coverage when pCO is slightly less than pO$_2$, whereas, at 485°K, the two are equal when pCO is slightly larger than pO$_2$.

Figures 9 and 3 may be overlaid to provide a comparison like that shown in Fig. 8. A detailed comparison reveals one apparent discrepancy—for pCO equal to pO$_2$, Fig. 8 indicates a much higher CO coverage at 453°K than at 485°K, which suggests that the rate at 453°K is much smaller than that at 485°K. Figure 3, however, indicates that the rates are about equal. This apparent discrepancy, which also arises when Figs. 1 and 3 are compared in detail, is related to the long-term stability of the carbon monoxide coverages (see below).

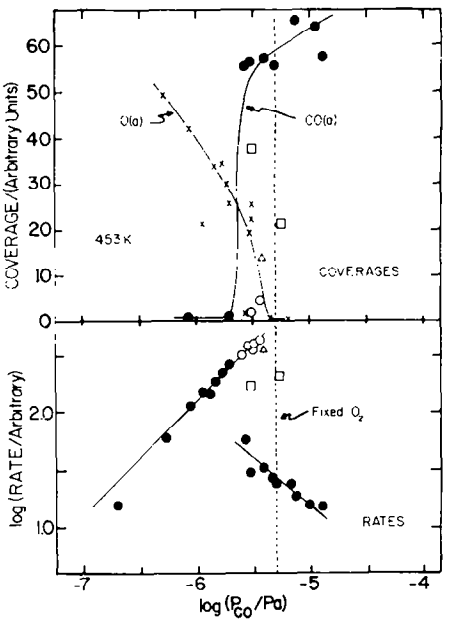

FIG. 10. *Lower panel:* CO_2 production rate as a function of CO pressure. The open symbols denote long-lived intermediate states. *Upper panel:* (X and △) oxygen coverages and CO (●, ○, and □) CO coverages in different and arbitrary units. The open symbols are associated with the same symbols in the lower panel.

Long-lived Metastable states

Below 485°K, and for pCO approximately equal to pO$_2$, the steady-state CO_2 production rates were difficult to establish because the system frequently achieved a metastable condition which persisted for at least 15 min before decaying to a stable steady state. As suggested by Fig. 10, and as will be further discussed, slowly varying carbon monoxide coverages are associated with these metastable states. The upper panel of Fig. 10 shows the carbon monoxide and oxygen coverages, and the lower panel shows the CO_2 production rates. The solid symbols denote stable steady states, and the open symbols denote metastable states. Open squares in the upper panel go with open squares in the lower panel, and so on. As indicated, the metastable states all appear when pCO equals pO$_2$ and can be prepared in at least two ways. In the first, the CO pressure is slowly increased from pCO much less than pO$_2$. As pCO approaches pO$_2$, high CO_2 production rates and low CO coverages result (open circles). In the second method, a stable steady state is prepared in the region where pCO

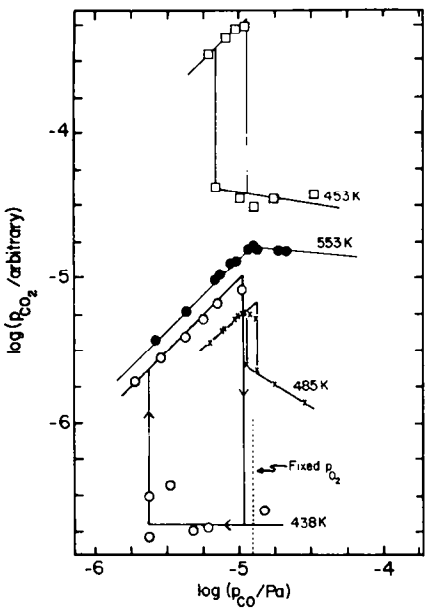

FIG. 11. CO_2 production rate as a function of CO pressure for a fixed O_2 pressure of 1.3×10^{-5} Pa. The ordinates have been arbitrarily shifted for clarity. Arrows give the sense of CO pressure and CO_2 rate variations.

is approximately equal to 2×10^{-6} Pa. The CO pressure is then raised (smoothly, quickly, and momentarily) into the high-pressure (10^{-5} Pa) region and reduced (quickly) to a value slightly less than the oxygen pressure. The resulting metastable rates and coverages typically lie in the gap region of Fig. 10, and three examples are shown (open squares and open triangles). These results indicate that carbon monoxide coverage is the important factor in determining the metastable rate. When CO coverage is very low, the rate is very high (open circles), and when it is intermediate the rate is intermediate (open squares). Furthermore, the accumulation of CO on the surface, in a form which inhibits the rate, does not immediately follow changes in the CO collision frequency. The open triangles of Fig. 10 denote a metastable state (prepared by the second method) for which oxygen coverage and rate were measured. The measured rate is near but below the maximum, and the oxygen coverage is about 20% of the maximum.

We have investigated the stability characteristics as a function of temperature, and Fig. 11 shows the results (the ordinates at various temperatures have been arbitrarily shifted for clarity). The states indicated were all stable for at least 15 min, and those in the inhibition region were stable for 1 hr, the longest measurement time. The four temperatures shown, 438, 453, 485, and 553°K, were all studied by cycling the CO pressure from low to high and then high to low values. At 553°K, the rate follows the same curve whether the CO pressure is increased or decreased. At 485, 453, and 438°K, however, a hysteresis loop appears. As the CO pressure is increased from low values, the rate increases smoothly to the point, which depends only slightly on the temperature, where it drops sharply into the inhibition region. When the CO pressure is slowly lowered, the rate follows the inhibition curve well into the region pCO less than pO$_2$ to another pressure point, where it increases sharply to high values on the first order curve. The lower limit point of the inhibition region drops sharply as the temperature is lowered. At 438, 453, and 485°K, the lower limits are at pCO/pO$_2$ equal to 0.2, 0.5, and 0.9, respectively. These may be compared to the values at which the rate maximizes (Fig. 2), pCO/pO$_2$ of 0.25, 0.4, and 1.0.

DISCUSSION

The steady-state rates shown in Figs. 1 through 8 as a function of pressure and temperature represent a complex interplay of oxygen and carbon monoxide adsorption, desorption, and reaction. Since CO_2 is only very weakly held on Pt (*46*), its adsorption–desorption properties will not influence the rate in these experiments. Work in our laboratory has shown that the initial sticking probability of oxygen on this polycrystalline foil is 0.36 (*23*, *101*). Between

300 and 550°K, the saturation amount of oxygen is nearly constant, but above about 600°K it drops off significantly. This is underscored by the results plotted in Fig. 12, which shows a flash desorption spectrum for O_2 after saturation of the Pt substrate with oxygen at 400°K and after evacuation. The production of CO_2 is sensitive to the rate at which adsorbed oxygen atoms are formed at the surface. In fact, if the only path for oxygen loss from the surface is reaction to form CO_2, then the rate of CO_2 production will equal the rate of oxygen atom formation at the surface. For temperatures above 600°K, Fig. 12 shows that desorption as O_2 also occurs and will compete with CO_2 production for adsorbed oxygen. According to Fig. 1, the competition becomes significant around 750°K, irrespective of the ratio of gas phase oxygen to carbon monoxide. At high temperatures, the rate may also decline because CO diffusion lengths are shorter. Since the activation energy for surface diffusion of CO is less than the activation energy for desorption, the number of sites sampled by a surface CO molecule will decrease as the temperature increases and can contribute to a declining rate. Another factor which may contribute is a declining CO sticking probability. For temperatures below 750°K, desorption of oxygen as O_2 is not a competitive process, and the rate can be interpreted in terms of a single path for oxygen removal —CO_2 production.

Over the range where there is no temperature dependence, T between 540 and 750°K, the rates at 620°K (Figs. 5 and 7) are typical. Setting pCO equal to $2p$O$_2$ as a reference, increasing pCO by a factor of 10 gives no significant increase in rate (Fig. 5). Setting pO$_2$ equal to $2p$CO as a reference, increasing pO$_2$ by a factor of 5 or 10 also gives no increase in rate (Fig. 7).

With the assumption made above, that the steady-state rate is equal to the rate of formation of oxygen atoms at the surface, and further assuming that CO reacts with

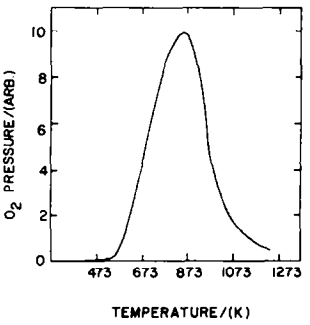

FIG. 12. Oxygen flash desorption spectrum.

O(a) while in a short-lived mobile precursor state and that the very small CO coverage has a negligible effect on the rate of oxygen adsorption, a simple explanation of the data over the intermediate temperature region can be given (*23*, *99*, *101*). This model assumes that all chemisorbed oxygen atoms are equally reactive and that CO in the mobile precursor state will collide and react with an adsorbed oxygen atom with high probability. The possibility that the oxygen reactivity depends on its coverage will be discussed in a later paper (*101*). When pCO is increased there is, near pCO equal to pO$_2$, a point where the coverage of oxygen reaches a very low value (see Fig. 9). In this situation, the O adsorption rate is highest and is balanced by the rate at which CO enters the mobile precursor state and reacts. Keeping the oxygen pressure constant and increasing the CO pressure by a factor of 5 gives no increase in the rate (See Fig. 1), because the adsorption of oxygen is rate determining and does not change as the CO pressure is increased. On the other hand, keeping the carbon monoxide pressure constant and increasing the oxygen pressure by a factor of 5 or 10 gives no increase in the rate, because the rate of CO entry into the mobile precursor state is now rate determining and does not change as the O_2 pressure is increased. Increasing the O_2 pressure will certainly give an increase in the oxygen coverage, but the pressure is already above a critical value

which makes the rate of entry of CO into the precursor state rate determining. According to the model, the oxygen coverage should rise until one-half the oxygen collision frequency times the coverage-dependent oxygen sticking coefficient equals the carbon monoxide collision frequency times the probability of entering the mobile precursor state.

Below 540°K, Fig. 1 indicates that the rate is dependent on the ratio of gas phase oxygen to carbon monoxide. When pCO/pO$_2$ equals 5, the relatively high CO pressure (and therefore collision frequency) and relatively low temperature makes possible the accumulation of chemisorbed carbon monoxide. This accumulation lowers both the steady-state oxygen coverage and the rate of oxygen adsorption. In this case, there are more than enough CO collisions to use all the oxygen that is chemisorbed, so oxygen adsorption is rate determining.

The mechanism of CO_2 production which is operative at steady state under these low temperatures and relatively high pCO conditions cannot be unambiguously established using our techniques. The presence of adsorbed CO, however, requires that the classical Langmuir–Hinshelwood mechanism be considered. On the other hand, the steady-state rate can be explained using an Eley–Rideal mechanism with CO reacting while in a mobile presursor state (*59, 99*). Both paths probably contribute, to varying degrees, in the region pCO greater than pO$_2$. A detailed discussion of this point is postponed (*101*).

The simplest interpretation of the sharp gaps in Figs. 3 and 4 involves the accumulation of CO which occurs once the rate of entry of CO into the mobile precursor state exceeds the maximum rate of production of oxygen atoms at the Pt surface. When the two rates are equal, no carbon monoxide will accumulate, but when the rate of entry into the mobile precursor state is larger, even slightly, CO will accumulate, and its concentration will be limited by the isotherm. This simple model agrees qualitatively with the data of Figs. 3, 4, 6, 8, and 9. Although the CO coverage under working conditions is not a step function of the CO pressure, it is a very steeply rising function. The curvature in the coverage of CO around pO$_2$ equal to pCO may arise from several sources, including nonuniform surface properties and participation of the LH path in the production of CO_2. The accumulation of CO at the surface results in a dramatic decline in the rate of O(a) formation because each CO(a) blocks one or more oxygen adsorption sites. Since it is limited by the oxygen adsorption rate, the CO_2 production rate drops sharply from its maximum value. The decrease in the magnitude of the gap with increasing temperature arises principally because the CO adsorption isotherm moves to lower coverages as the temperature is increased. At 620 and 540°K (Figs. 5 and 8), there is no gap, and the rate stays near its maximum when the rate at which CO enters the mobile precursor state exceeds the rate of O(a) formation.

The data of Figs. 1, 2, and 11 are related as indicated in the Results section. That is, the gap position occurs at a well-defined pCO/pO$_2$ and T. Only a small extension of the simple collision frequency model is required to order to account for these results. If the temperature is low enough for significant amounts of CO to accumulate in the absence of reaction, then, for some critical ratio of the CO and O_2 collision frequencies, the oxygen coverage drops to a value which makes it possible for CO in the precursor state to chemisorb rather than react. Assuming that chemisorbed carbon monoxide is slightly less reactive than precursor carbon monoxide for either activation energy or steric reasons, it will accumulate (and the oxygen adsorption rate will drop) until the coverage either reaches a value near the equilibrium isotherm or is limited by removal through the LH pathway. As the temperature is lowered,

CO chemisorption becomes competitive with reaction at lower pCO/pO_2, and, as a result, the oxygen adsorption and CO_2 production rates plummet for lower relative CO pressures (Fig. 11). Contrariwise, as pCO/pO_2 is lowered the temperature at which the gap occurs drops (Fig. 1). As noted in the Results section, the correlation between the (temperature, pCO/pO_2) pair determined by working at fixed pCO/pO_2 and varying T (Figs. 1 and 2) and the pair determined by varying pCO/pO_2 at constant T (Fig. 11) is excellent.

Gaps in the CO_2 production rate have been observed in high pressure CO/O_2 Pt systems (*94*, *95*). For example, at pressures in the Torr region and at T equal to 460°K, Cochran *et al.* [83] observed a drop of approximately a factor of 4 in the CO_2 production rate around pCO/pO_2 equal to 0.1, which is a much lower ratio than that reported here. This may be due to Pt surface structure differences which effect the oxygen adsorption rate. Another possibility, which will be briefly considered here, is that there is a weak dependence on the CO collision frequency.

The sharp drop in CO_2 production is associated with a sharp increase in the carbon monoxide coverage. In the above discussion, only relative CO and O_2 collision frequencies have been considered. At high absolute CO collision frequencies (high pressures), however, surface structures may appear, even in the presence of oxygen, which either do not form when pCO/pO_2 is much less than 1 and pCO is low or appear with statistically insignificant probability. If these structures significantly lower the oxygen adsorption rate, then the gap could well move to lower pCO/pO_2, as observed. Candidate structures would include islands of weakly held carbon monoxide within which CO is very unreactive.

One final point remains to be discussed. Around the gap region, the most stable state is established when the temperature is below 485°K and the gap region is approached very slowly by increasing the pCO. It is attractive to suppose that certain CO structures must form before accumulation and inhibition can occur. At low pCO, these either do not form or, in the presence of relatively high pO_2, are controlled by adsorbed oxygen in a way which prevents CO accumulation. The latter is the more probable, considering the relative lack of sensitivity to pCO. As pCO is increased to the point where adsorbed CO can accumulate, the formation of the required structures is slow compared to oxygen adsorption and reaction to form CO_2. One possible structure might be an organized group of several CO molecules which would serve as the nucleus for the growth of an island of CO.

SUMMARY

These results suggest that, over a wide range of temperatures and low pressures, the CO oxidation reaction on polycrystalline platinum can be described in terms of a model which involves weakly held precursor CO molecules reacting with chemisorbed oxygen atoms to form CO_2. At temperatures above 750°K, desorption of O_2 and CO diffusion lengths becomes an important factor, and the rate drops. In the range below 540°K, and depending strongly on pCO/pO_2, there is a temperature below which the rate falls sharply. Coverage measurements indicate the low rates are associated with high CO and low O coverages. In this region, some CO_2 may be formed by reaction between adsorbed CO and adsorbed oxygen. The same conclusions are reached on the basis of steady-state rate measurements at fixed T and pO_2 and variable pCO. At temperatures below 540°K, and over a very narrow range of pressures, sharp drops, associated with the accumulation of CO, appear in the CO_2 production rate. Under some conditions, states are formed which have unusually high CO_2 production rates but which are

metastable and decay slowly to states in the inhibition region. The relatively long time required for the decay may be associated with the formation of organized structures of adsorbed CO on the surface.

REFERENCES

1. Collins, D. M., Lee, J. B., and Spicer, W. E., *Surf. Sci.* **55**, 389 (1976).
2. Norton, P. R., *Surf. Sci.* **47**, 98 (1975).
3. Nishiyama, Y., and Wise, H., *J. Catal.* **32**, 50 (1974).
4. Procop, M., and Völter, J., *Z. Phys. Chem. (Leipzig)* **250**, 387 (1972).
5. Völter, J., Procop, M., and Berndt, H., *Surf. Sci.* **39**, 453 (1973).
6. Peng, Y. K., and Dawson, P. T., *Canad. J. Chem.* **52**, 3507 (1974).
7. Wood, B. J., Endow, N., and Wise, H., *J. Catal.* **18**, 70 (1970).
8. Alnot, M., Cassuto, A., Fusy, J., and Pentenero, A., paper presented at the Proc. 2nd Internat. Conf. on Solid Surfaces, 1974.
9. Weber, B., Fusy, J., and Cassuto, A., *J. Chem. Phys.* **66**, 708 (1969).
10. Kneringer, G., and Netzer, F. P., *Surf. Sci.* **49**, 125 (1975).
11. Wilf, M., and Dawson, P. T., *Surf. Sci.* **65**, 399 (1977).
12. Blakely, D. W., and Somorjai, G. A., *Surf. Sci.* **65**, 419 (1977).
13. Lang, B., Joyner, R. W., and Somorjai, G. A., *Surf. Sci.* **30**, 454 (1972).
14. Morgan, A. E., and Somorjai, G. A., *Surf. Sci.* **12**, 405 (1968).
15. Bonzel, H. P., and Ku, R., *Surf. Sci.* **33**, 91 (1972).
16. Joebstl, J. A., *J. Vac. Sci. Technol.* **12**, 347 (1975).
17. Ducros, R., and Merrill, R. P., *Surf. Sci.* **55**, 227 (1976).
18. Carriere, B., Legare, P., and Maire, G., *J. Chim. Phys.* **71**, 355 (1974).
19. Carriere, B., Deville, J. P., Maire, G., and Legare, P., *Surf. Sci.* **58**, 618 (1976).
20. Lang, B., Legare, P., and Maire, G., *Surf. Sci.* **47**, 89 (1975).
21. Bonzel, H. P., and Ku, R., *Surf. Sci.* **40**, 85 (1973).
22. Helms, C. R., Bonzel, H. P., and Kelemen, S., *J. Chem. Phys.* **65**, 1773 (1976).
23. Matsushima, T., Almy, D. B., and White, J. M., *Surf. Sci.* **67**, 89 (1977).
24. Hopster, H., Ibach, H., and Comsa, G., *J. Catal.* **46**, 37 (1977).
25. Pignet, T. P., Schmidt, L. S., and Jarvis, N. L., *J. Catal.* **31**, 145 (1973).
26. Weinberg, W. H., Lambert, R. M., Comrie, C. M., and Linnett, J. W., *Surf. Sci.* **39**, 456 (1973).
27. Norton, P. R., *J. Catal.* **36**, 211 (1975).
28. Norton, P. R., Tapping, R. L., and Goodale, J. W., *J. Vac. Sci. Technol.* **14**, 446 (1977).
29. Norton, P. R., and Richards, P. J., *Surf. Sci.* **49**, 567 (1975).
30. Collins, D. M., Lee, J. B., and Spicer, W. E., *Phys. Rev. Lett.* **35**, 592 (1975).
31. Gorodetski, V. V., and Savchenko, V. I., *in* Proc. 5th Inter. Congr. on Catalysis, 1972, J. Hightower, Ed., p. 527.
32. Lewis, R., and Gomer, R., *Surf. Sci.* **12**, 157 (1968).
33. Stoll, A. G., Jr., and Merrill, R. P., to be published.
34. Pacia, N., Weber, B., and Pentenero, A., *Surf. Sci.* **49**, 330 (1975).
35. Pacia, N., Weber, B., and Pentenero, A., *J. Chim. Phys.* **72**, 945 (1975).
36. Palmer, R. L., *J. Vac. Sci. Technol.* **12**, 1403 (1975).
37. Benson, J. E., and Boudart, M., *J. Catal.* **4**, 704 (1965).
38. Mears, D. E., and Hansford, R. C., *J. Catal.* **9**, 125 (1967).
39. Kikuchi, E., Flynn, P. C., and Wanke, S. E., *J. Catal.* **34**, 132 (1974).
40. Wentrcek, P., Kimoto, K., and Wise, H., *J. Catal.* **33**, 279 (1973).
41. Morrow, B. A., and Ramamurthy, P., *J. Phys. Chem.* **77**, 3052 (1973).
42. Weinberg, W. H., Lambert, R. M., Comrie, C. M., and Linnett, J. W., *Surf. Sci.* **30**, 299 (1972).
43. Weinberg, W. H., and Merrill, R. P., *Surf. Sci.* **39**, 206 (1973).
44. Boudart, M., Collins, D. M., Hanson, F. V., and Spicer, W. E., *J. Vac. Sci. Technol.* **14**, 441 (1977).
45. Miyazaki, E., and Yasumori, I., *Surf. Sci.* **55**, 747 (1976).
46. Norton, P. R., *Surf. Sci.* **44**, 624 (1974).
47. Langmuir, I., *Trans. Faraday Soc.* **17**, 621 (1922).
48. Bonzel, H. P., and Ku, R., *J. Vac. Sci. Technol.* **9**, 663 (1972).
49. Bonzel, H. P., and Ku, R., *J. Chem. Phys.* **59**, 1641 (1973).
50. Bonzel, H. P., and Burton, J. J., *Surf. Sci.* **52**, 223 (1975).
51. Hori, G. K., and Schmidt, L. D., *J. Catal.* **38**, 335 (1975).
52. Sklyarov, A. V., Tret'yakov, I. I., Shule, B. R.,

and Roginskii, S. Z., *Dokl. Akad. Nauk SSSR* **189**, 1302 (1969).
53. McCarthy, E., Zahradnik, J., Kuczynski, G. C., and Carberry, J. J., *J. Catal.* **39**, 29 (1972).
54. Winterbottom, W. L., *Surf. Sci.* **36**, 205 (1973).
55. Freel, J., *J. Catal.* **25**, 139 (1972).
56. Alnot, M., Fusy, J., and Cassuto, A., *Surf. Sci.* **57**, 651 (1976).
57. Pacia, N., Cassuto, A., Pentenero, A., and Weber, B., *J. Catal.* **41**, 455 (1976).
58. Palmer, R. L., and Smith, J. N., Jr., *J. Chem. Phys.* **60**, 1453 (1974).
59. White, J. M., and Golchet, A., *J. Chem. Phys.* **66**, 5744 (1977).
60. Dagonnier, R., and Nuyts, J., *J. Chem. Phys.* **65**, 2061 (1976).
61. Wentreek, P., and Wise, H., *J. Catal.* **36**, 247 (1975).
62. Ertl, G., Neumann, M., and Streit, K. M., *Surf. Sci.* **64**, 393 (1977).
63. Lambert, R. M., *Surf. Sci.* **49**, 325 (1975).
64. Clarke, T. A., Mason, R., and Tescari, M., *Proc. R. Soc. London Ser. A* **331**, 321 (1972).
65. Netzer, F. P., and Matthew, J. A. D., *Surf. Sci.* **51**, 352 (1975).
66. Morgan, A. E., and Somorjai, G. A., *J. Chem. Phys.* **51**, 3309 (1969).
67. Tucker, C. W., Jr., *Surf. Sci.* **2**, 516 (1964).
68. Comrie, C. M., and Lambert, R. M., *J. Chem. Soc. Faraday Trans. I* **72**, 1659 (1976).
69. Lewis, R., and Gomer, R., *Nuovo Cimento (Suppl.)* **5**, 506 (1967).
70. Gorodetskii, V. V., and Savchenko, V. I., *Dokl. Phys. Chem.* **215**, 271 (1974).
71. Primet, M., Basset, J. M., Mathieu, M. V., and Prettre, M., *J. Catal.* **29**, 213 (1973).
72. Eischens, R. P., and Plinskin, W. A., *Adv. Catal.* **10** (1958).
73. Eischens, R. P., Francis, S. A., and Plinskin, W. A., *J. Phys. Chem.* **60**, 194 (1956).
74. Hoffmann, F. M., and Bradshaw, A. M., *J. Catal.* **44**, 328 (1976).
75. Shigeishi, R. A., and King, D. A., *Surf. Sci.* **58**, 379 (1976).
76. Heyne, H., and Tompkins, F. C., *Proc. Roy. Soc. London Ser. A* **292**, 460 (1966).
77. Froitzheim, H., Hopster, H., Ibach, H., and Lehwald, S., *Appl. Phys.* **13**, 147 (1977).
78. Bonzel, H. P., and Fischer, T. E., *Surf. Sci.* **51**, 213 (1975).
79. Clarke, T. A., Gay, I. D., Law, B., and Mason, R., *Chem. Phys. Lett.* **31**, 29 (1975).
80. Iwasawa, Y., Mason, R., Textor, M., and Somorjai, G. A., *Chem. Phys. Lett.* **44**, 468 (1976).
81. Bouwman, R., and Sachtler, W. M. H., *J. Catal.* **26**, 63 (1972).
82. Miller, J. N., Ling, D. T., Lindau, I., Stefan, P. M., and Spicer, W. E., *Phys. Rev. Lett.* **38**, 1419 (1977).
83. Apai, G., Wehner, P. S., Williams, R. S., Stohr, J., and Shirley, O. A., *Phys. Rev. Lett.* **37**, 1498 (1976).
84. Grant, J. T., and Hooker, M. P., *J. Elect. Spectrosc. Relat. Phenom.* **9**, 93 (1976).
85. Hooker, M. P., and Grant, J. T., *Surf. Sci.* **62**, 21 (1977).
86. Martinez, J. M., and Hudson, J. B., *J. Vac. Sci. Technol.* **10**, 35 (1973).
87. Lambert, R. M., and Comrie, C. M., *Surf. Sci.* **38**, 197 (1973).
88. McCabe, R. W., and Schmidt, L. D., *Surf. Sci.* **60**, 85 (1976).
89. McCabe, R. W., and Schmidt, L. D., *Surf. Sci.* **66**, 101 (1977).
90. Stephan, J. J., and Ponec, V., *J. Catal.* **42**, 1 (1976).
91. Winterbottom, W. L., *Surf. Sci.* **37**, 195 (1973).
92. Rockova, E., *J. Catal.* **48**, 150 (1977).
93. Doyen, G., and Ertl, G., *Surf. Sci.* **43**, 197–229 (1974).
94. Dauchot, J. P., and Van Cakenberghe, J., Proc. 2nd Interml. Conf. on Solid Surfaces, p. 533, 1974.
95. Cochran, H. D., Donnelly, R. G., Modell, M., and Baddour, R. F., Colloid and Interface Science, Vol. 3, (M. Kerker, Ed.), Academic Press, New York, 1977.
96. Hugo, P., and Jakubith, M., *Chem. Ing. Technol.* **44**, 383 (1972).
97. Wei, J., *Adv. Catal.* **24**, 57 (1975).
98. Skinner, G. B., "Introduction to Chemical Kinetics," p. 154, Academic Press, New York, 1974.
99. Palmer, R. L., *Catal. Rev.-Sci. Eng.* **12**, 279 (1975).
100. Weinberg, W. H., *J. Catal.* **40**, 268 (1975).
101. Golchet, A., Turner, J. S., and White, J. M., to be published.
102. Flaim, T. A., and Ownby, P. D., *J. Vac. Sci. Technol.* **8**, 661 (1971).
103. Ertl, G., and Koch, J., Second International Symposium on Adsorption-Desorption Phenomena, Florence, 1971.
104. Ertl, G., and Rau, P., *Surf. Sci.* **15**, 443 (1969).
105. Close, J. S., and White, J. M., *J. Catal.* **36**, 185 (1975).
106. Matsushima, T., Almy, D. B., Foyt, D. C., Close, J. S., and White, J. M., *J. Catal.* **39**, 277 (1975).